Supporting Information

The NBD tertiary amine is a fluorescent quencher and/or a weak green-light fluorophore in H_2S-specific probes

Ruirui Chen,[†a] Haishun Ye,[†b] Tian Fang,[a] Shanshan Liu,[b] Long Yi,*[b] and Longhuai Cheng*[a]

[a]State Key Laboratory of Elemento-Organic Chemistry and Department of Chemical Biology, College of Chemistry, National Engineering Research Center of Pesticide, Nankai University, Tianjin 300071, China. Email: chenglonghuai@nankai.edu.cn
[b]State Key Laboratory of Organic-Inorganic Composites and Beijing Key Lab of Bioprocess, Beijing University of Chemical Technology (BUCT), 15 Beisanhuan East Road, Chaoyang District, Beijing 100029, China. Email: yilong@mail.buct.edu.cn
[†]These authors contributed equally to this work.

Table of contents

1. Reagents and instruments

All chemicals used for synthesis were purchased from commercial suppliers and applied directly without further purification. Merck silica gel 60 (70−200 mesh) was used for general column chromatography purification. ^{1}H NMR and ^{13}C NMR spectra were recorded on a Bruker 400 NMR spectrometer. High-resolution mass spectra (HRMS) were recorded on an Agilent 6540 UHD Accurate Mass Q-TOFLC/MS. The UV−visible spectra were recorded on a UV-6000 UV−vis-NIR-spectrophotometer. Fluorescence studies were performed using F-280 spectrophotometer. The cellular bioimaging was carried out on confocal microscopes (Olympus FV 1000).

2. Synthetic procedure of compounds

Compounds **NBD-NHEt**, **NBD-N(Et)$_2$** and **NBD-PZ** were synthesized based on our previous work.[1] For **NBD-NHEt**, ^{1}H NMR (400 MHz, DMSO-d_6) δ 9.51 (s, 1H), 8.49 (d, J = 8.8 Hz, 1H), 6.38 (d, J = 9.0 Hz, 1H), 3.59–3.41 (m, 2H), 1.27 (t, J = 7.2 Hz, 3H); ^{13}C NMR (101 MHz, DMSO-d_6) δ 144.9, 144.3, 144.1, 137.8, 120.5, 98.9, 38.2, 13.2. HRMS (ESI): m/z [M]$^+$ calcd. for $C_8H_9N_4O_3^+$: 209.0669; found: 209.0653. For **NBD-N(Et)$_2$**, ^{1}H NMR (400 MHz, DMSO-d_6) δ 8.41 (d, J = 9.3 Hz, 1H), 6.43 (d, J = 9.3 Hz, 1H), 4.13–3.80 (m, 4H), 1.30 (t, J = 7.1 Hz, 6H); ^{13}C NMR (101 MHz, DMSO-d_6) δ 144.8, 144.1, 136.2, 119.5, 101.9, 47.8, 12.2. HRMS (ESI): m/z [M]$^+$ calcd. for $C_{10}H_{13}N_4O_3^+$: 237.0982; found: 237.0978. For **NBD-PZ**, ^{1}H NMR (400 MHz, DMSO-d_6) δ 8.45 (d, J = 9.2 Hz, 1H), 6.64 (d, J = 9.3 Hz, 1H), 4.14–4.02 (m, 4H), 2.99–2.89 (m, 4H).

Synthesis of NBD-PZ-TPP. 4-Carboxybutyltriphenylphosphonium bromide (266 mg, 0.6 mmol) was dissolved in 5 mL DMF, then HATU (228 mg, 0.6 mmol) and DMAP (147 mg, 1.2 mmol) were added to the solution. After stirring for 10 min, **NBD-PZ** (125 mg, 0.5 mmol) was added to the solution.[1] The mixture was stirred at room temperature overnight, and the solvent was

removed under reduced pressure, and the resulted residue was purified by silica gel column chromatography to give an oil **NBD-PZ-TPP** (254 mg, yield 73%). ^{1}H NMR (400 MHz, DMSO-*d*6) δ 8.51 (d, *J* = 9.1 Hz, 1H), 7.95–7.87 (m, 3H), 7.85–7.75 (m, 12H), 6.60 (d, *J* = 9.2 Hz, 1H), 4.27–4.16 (m, 2H), 4.16–4.05 (m, 2H), 3.80–3.68 (m, 4H), 3.68–3.54 (m, 2H), 2.45 (t, *J* = 7.1 Hz, 2H), 1.82–1.69 (m, 2H), 1.68–1.54 (m, 2H); ^{13}C NMR (101 MHz, DMSO-*d*6) δ 170.6, 145.4, 144.8, 136.3, 134.9, 133.6, 130.3, 121.2, 119.0, 118.1, 103.1, 48.9, 43.4, 31.2, 25.4, 21.5, 20.3, 19.9. HRMS (ESI): m/z $[M]^+$ calcd. for $C_{33}H_{33}N_5O_4P^+$: 594.2265; found: 594.2280.

Synthesis of NBD-NH-TPP. A mixture of *N*-boc-ethylenediamine (320 mg, 2.0 mmol) and NBD-Cl (200 mg, 1.0 mmol) was dissolved in 10 mL dry DCM. DIPEA (0.34 mL, 2.0 mmol) was added to the reaction mixture. After stirring at room temperature for 3 h, the resulting solution was evaporated by distillation under reduced pressure. The residue was purified by flash column chromatography eluting to give a solid product (255 mg, 79%), which was treated with CH_2Cl_2 (3 mL) and trifluoroacetic acid (TFA, 1 mL) at room temperature 1 h. The solvent and TFA were removed under reduced pressure to give NBD-ethylenediamine without further purification. Compound NBD-ethylenediamine (0.5 mmol) was redissolved in anhydrous DMF (5 mL), and (4-carboxybutyl)triphenylphosphonium bromide (266 mg, 0.6 mmol), HATU (228 mg, 0.6 mmol) and DMAP (245 mg, 2.0 mmol) were added to the solution. The mixture was stirred at room temperature overnight, and the solvent was removed under reduced pressure. The resulted residue was purified by silica gel column chromatography to give **NBD-NH-TPP** (210 mg, yield 65%). ^{1}H NMR (400 MHz, DMSO-d_6) δ 9.39 (s, 1H), 8.52 (d, *J* = 8.7 Hz, 1H), 8.02 (t, *J* = 5.6 Hz, 1H), 7.93–7.85 (m, 3H), 7.82–7.72 (m, 12H), 6.39 (d, *J* = 9.0 Hz, 1H), 3.63–3.52 (m, 2H), 3.52–3.41 (m, 2H), 3.34–3.26 (s, 2H), 2.12 (t, *J* = 7.1 Hz, 2H), 1.76–1.64 (m, 2H), 1.59–1.45 (m, 2H); ^{13}C NMR (101 MHz, DMSO-d_6) δ 172.3, 164.6, 145.3, 137.9, 134.9, 133.6, 130.3, 120.9, 118.9, 118.0, 99.1, 43.1, 37.2, 34.2, 26.0, 21.3, 20.2, 19.7. HRMS (ESI): m/z $[M]^+$ calcd. for $C_{31}H_{31}N_5O_4P^+$: 568.2108; found: 568.2105.

3. Solubility test

The water solubility was tested by concentration-dependent absorbance spectra of of compounds **NBD-NHEt**, **NBD-N(Et)$_2$**, **NBD-PZ-TPP** and **NBD-NH-TPP** in PBS (50 mM, pH = 7.4), respectively. The plots of absorbance intensity at different absorption wavelength (348 nm, 360 nm, 351 nm, 345 nm) against the dye concentration were linear at low concentration and showed downward curvature at higher concentration. The maximum concentration in the linear region was considered as the solubility.[2]

4. General procedure for spectroscopic studies

All measurements were performed in degassed phosphate buffer (PBS, 50 mM, pH 7.4). Compounds were dissolved into DMSO to prepare the stock solutions with concentrations of 1-20 mM. Various stock solutions (100 mM) of different analytes were prepared in deionized water. The reaction mixture was shaken uniformly before spectra were measured. All measurements were performed in a 3 mL corvette with 2 mL solution at room temperature or 25 °C and all the fluorescence spectra were obtained by excitation at 493 nm.

5. Quantum yield

The quantum yields of **NBD-NHEt** and **NBD-N(Et)$_2$** in various solvents and the quantum yields of **NBD-PZ-TPP** and **NBD-NH-TPP** in PBS (50 mM, pH = 7.4) were measured with rhodamine B in ethanol as the standard (Φ = 0.89).[3] The excitation wavelength was at 495 nm, and the emission range was 500-650 nm. The quantum yield was calculated using the following equation:

$$\Phi = \Phi_S \times (F/F_S) \times (A_S/A) \times (n^2/n_S^2)$$

where Φ is the quantum yield, A is the absorbance at the excitation wavelength, F is the area under the corrected emission curve, and n is the refractive index of the solvents used. Subscript S refers to the standard.

6. Cell culture and MTT assay

HeLa cells (human cervical cancer cells) were cultured at 37 ºC, 5% CO_2 in DMEM/HIGH GLUCOSE (GIBICO) supplemented with 10% fetal bovine serum (FBS), 100 U/mL penicillin, 100 μg/mL streptomycin, and 4 mM L-glutamine. The HeLa cells were passaged every 2 days under standard cell culture conditions and used between passages 3 and 8, and then seeded in the 96-well plate at the density about 1×10^4/well. After 24 h of cultivation, the culture medium of HeLa cells was replaced with a fresh one containing different concentrations of probe **NBD-PZ-TPP** or **NBD-NH-TPP** (0, 5, 10, 20, 30, 40 and 50 μM) and then incubated for another 24 h. Then, 5 mg/mL MTT in PBS (20 μL) was added to each well and incubated for another 4 h. Finally, the culture medium was replaced with 150 μL of DMSO to dissolve the purple formazan crystals. The absorbance intensity in each well was detected at 490 nm by a microplate spectrophotometer (SpectraMax M2E (Molecular Device, Inc.)).

7. Imaging in living cell

HeLa cells seeded in the 12-well glass bottom plate at the density about 1×10^5/well and cultured for 12 h under standard cell culture conditions. After that, the culture medium of HeLa cells was replaced with a fresh one containing different concentrations of probe **NBD-PZ-TPP** or **NBD-NH-TPP** (2, 5 and 10 μM) and then incubated for 1 h. After incubation, the cells were quickly washed with PBS, and then fixed with 4% paraformaldehyde solution for 10 min. After that, the cells were washed with PBS and then treated with DAPI (2 μg/mL) for 10 min. Finally, the HeLa cells were washed using PBS and imaged using a confocal microscope (Olympus FV1000) with a 40 × objective lens. The emission of probe was collected at the green channel (500-550 nm) with 488 nm excitation. DAPI stained HeLa cells were observed through the blue channel (450-500 nm) with 405 nm excitation. For excitation wavelength

imaging, HeLa cells in the 12-well glass bottom plate were incubated with 10 μM **NBD-PZ-TPP** for 60 min. After incubation, the cells were quickly washed with PBS, and then fixed with 4% paraformaldehyde solution for 10 min. Finally, the HeLa cells were washed using PBS and imaged using a confocal microscope (Olympus FV1000) with a 40 × objective lens. The emission of probe was collected at the different channel with 488/454/404 nm excitation. For the exogenous H_2S bioimaging, HeLa cells were pre-incubated with 200 μM Na_2S for 30 min, then washed and incubated with 10 μM **NBD-PZ-TPP** for 60 min. After that, the HeLa cells were incubated with Mito Tracker Deep Red FM (0.5 μM) for 30 min. After incubation, the cell s were quickly washed with PBS, and then fixed with 4% paraformaldehyde solution for 10 min. Finally, the HeLa cells were washed using PBS and imaged using a confocal microscope (Olympus FV1000) with a 40 × objective lens. The emission of probe was collected at the green channel (500-550 nm) with 488 nm excitation.

8. Supplementary figures

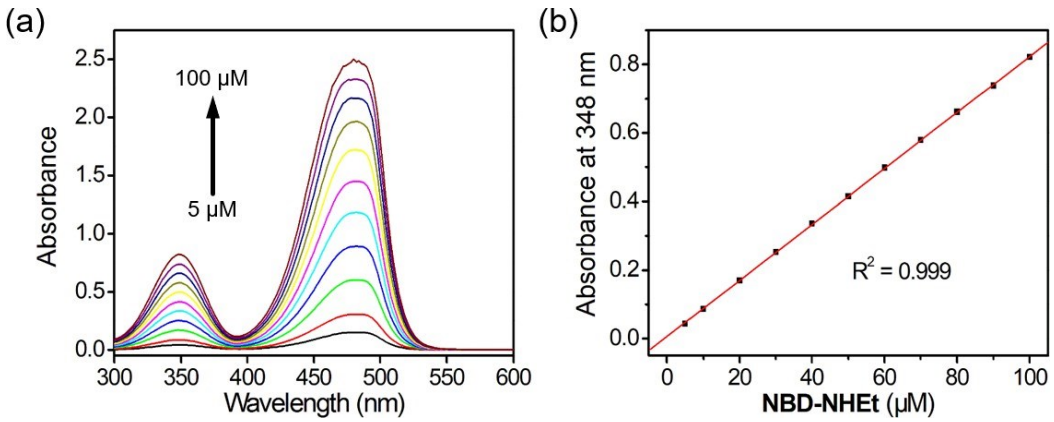

Fig. S1 Solubility analysis of **NBD-NHEt**. (a) The absorption spectra of **NBD-NHEt** at different concentrations in PBS buffer (50 mM, pH = 7.4). (b) The linear relationship of absorbance intensity at 348 nm and the concentration of **NBD-NHEt**.

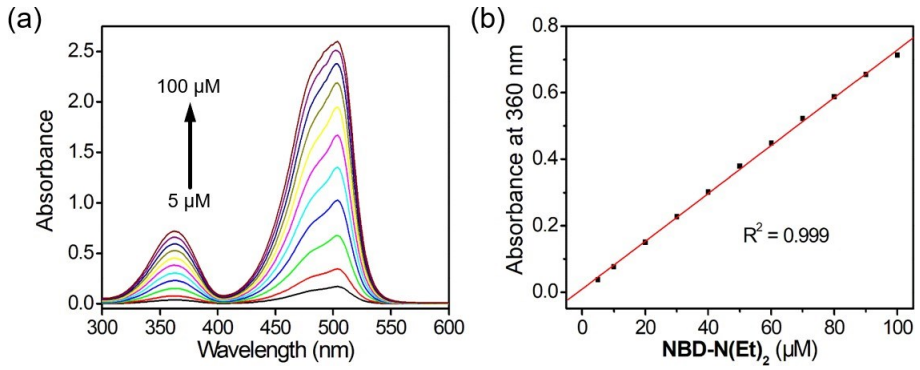

Fig. S2 Solubility analysis of **NBD-N(Et)$_2$**. (a) The absorption spectra of **NBD-N(Et)$_2$** at different concentrations in PBS buffer (50 mM, pH = 7.4). (b) The linear relationship of absorbance intensity at 348 nm and the concentration of **NBD-N(Et)$_2$**.

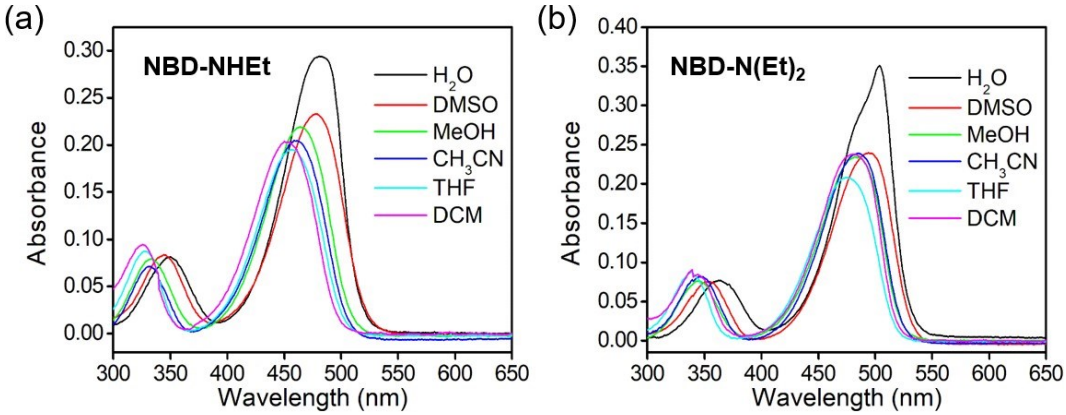

Fig. S3 (a, b) The absorption spectra of **NBD-NHEt** (10 μM) or **NBD-N(Et)$_2$** (10 μM) in various solvents, respectively.

Compound	Solvent	λ_{abs} (nm)	ε ($L \cdot mol^{-1} \cdot cm^{-1}$)	λ_{em} (nm)	Φ
NBD-NHEt	H_2O	482	29370	552	0.045
	DMSO	479	23275	540	0.637
	MeOH	464	21888	533	0.362
	CH_3CN	463	20401	527	0.769
	THF	456	19494	518	0.974
	DCM	452	20285	517	0.934
NBD-N(Et)$_2$	H_2O	504	35085	561	0.009
	DMSO	495	23908	548	0.028
	MeOH	483	23391	542	0.020
	CH_3CN	485	23885	539	0.019
	THF	476	20760	528	0.050
	DCM	482	23779	528	0.053

Table S1 Photophysical properties of **NBD-NHEt** and **NBD-N(Et)$_2$** in different solvents. Maximum absorbance, λ_{abs}; molar extinction coefficient, ε; emission, λ_{em}; quantum yields, Φ.

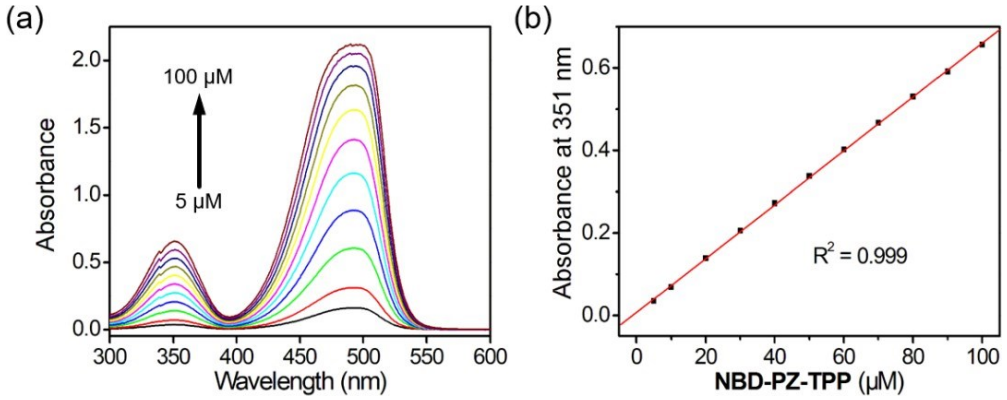

Fig. S4 Solubility analysis of **NBD-PZ-TPP**. (a) Concentration-dependent absorption spectra of **NBD-PZ-TPP** in PBS buffer (50 mM, pH = 7.4). (b) The linear relationship of absorbance intensity at 348 nm and the concentration of **NBD-PZ-TPP**.

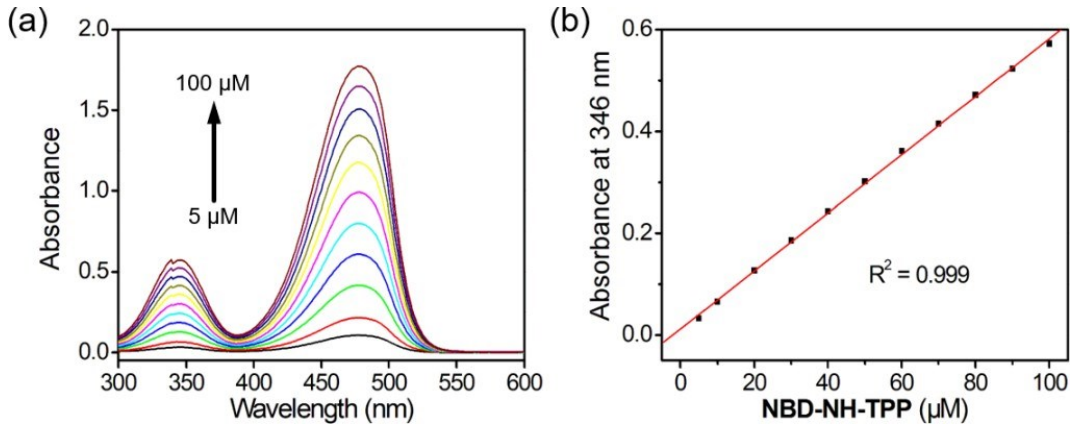

Fig. S5 Solubility analysis of **NBD-NH-TPP**. (a) Concentration-dependent absorption spectra of **NBD-NH-TPP** in PBS buffer (50 mM, pH = 7.4). (b) The linear relationship of absorbance intensity at 348 nm and the concentration of **NBD-NH-TPP**.

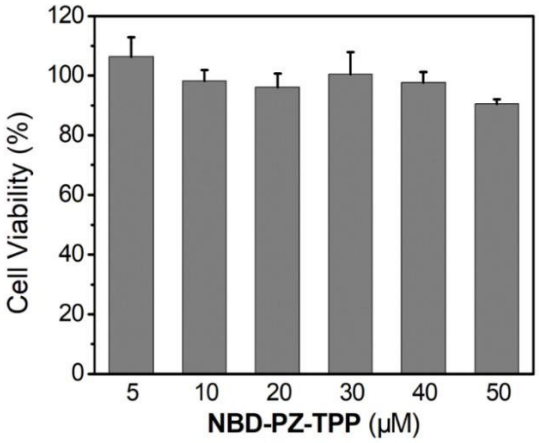

Fig. S6 Relative cell viability studies of **NBD-PZ-TPP** with HeLa cells for 24 h incubation by using the MTT assay. The results are expressed as mean ± SD (n = 3).

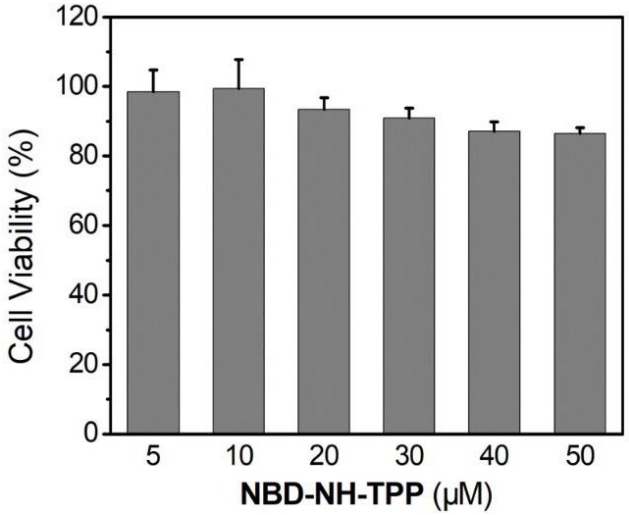

Fig. S7 Relative cell viability studies of probe **NBD-NH-TPP** with HeLa cells for 24 h incubation by using the MTT assay. The results are expressed as mean ± SD (n = 3).

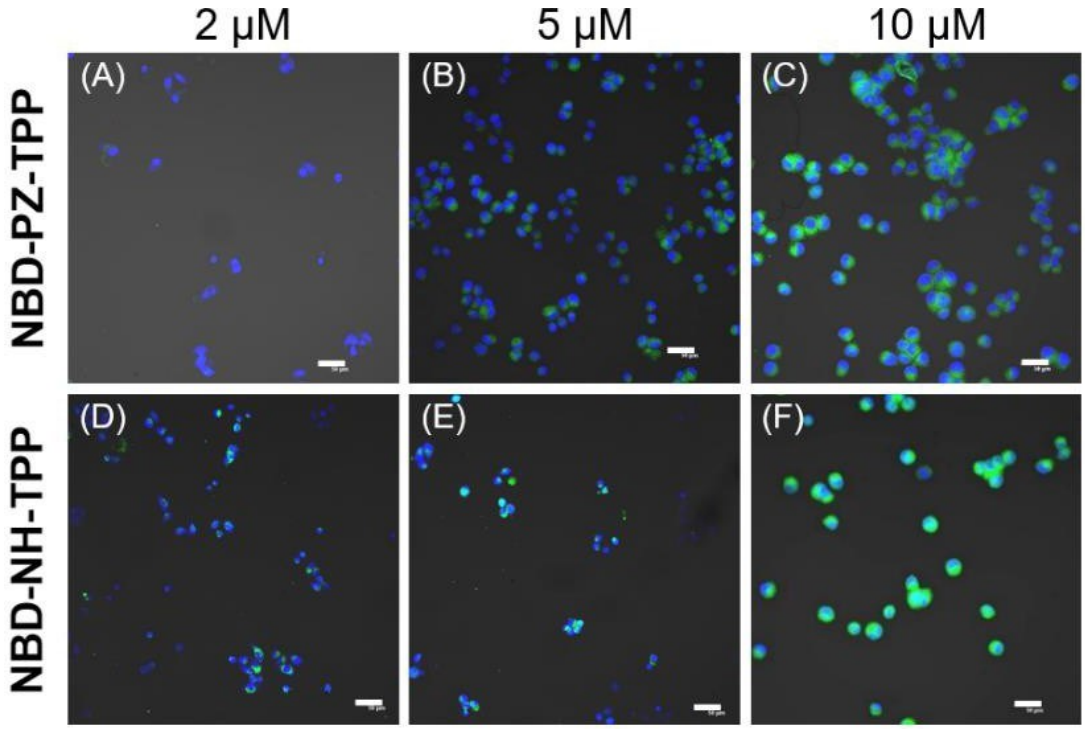

Fig. S8 Concentration-dependent merge images of blue fluorescence of DAPI and green fluorescent of probe **NBD-PZ-TPP** and **NBD-NH-TPP**, respectively.

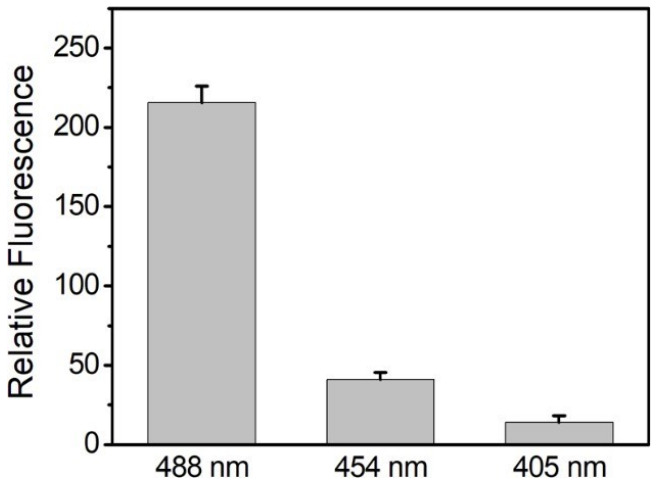

Fig. S9 Relative green fluorescence of images from Fig. 4, $N = 3$ fields of cells, error bars are means ± S.D.

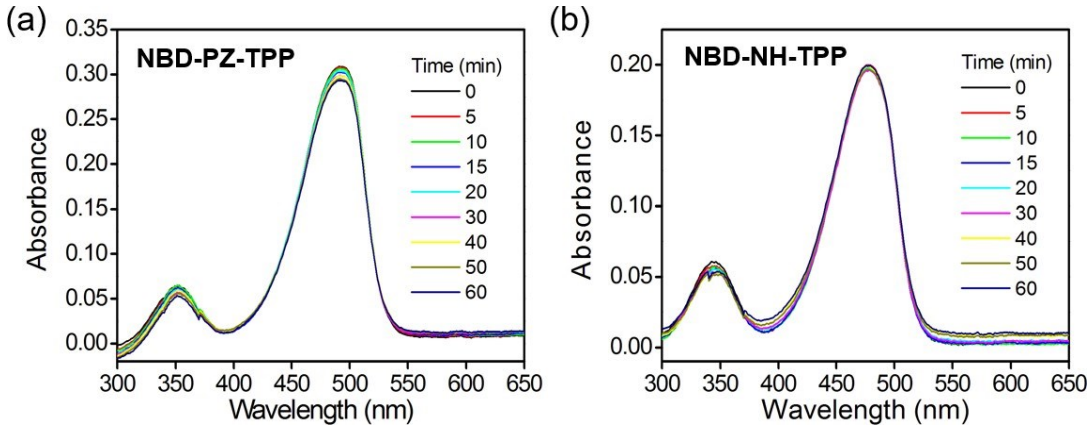

Fig. S10 (a, b) Time-dependent absorbance spectra of 10 μM **NBD-PZ-TPP** or **NBD-NH-TPP** towards 1.0 mM GSH in PBS buffer (50 mM, pH = 7.4) at 25 °C, respectively.

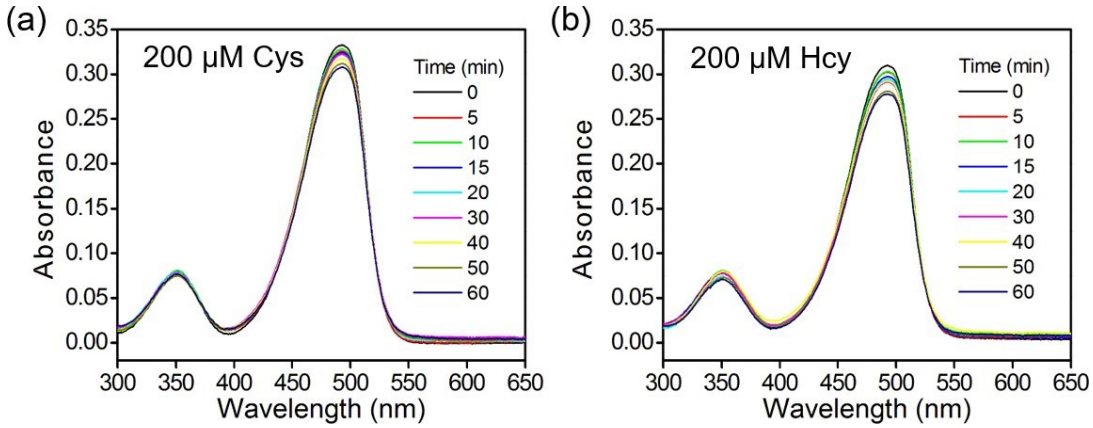

Fig. S11 Time-dependent absorbance spectra of 10 μM **NBD-PZ-TPP** towards 200 μM Cys (a) or 200 μM Hcy (b) in PBS buffer (50 mM, pH = 7.4) at 25 °C, respectively.

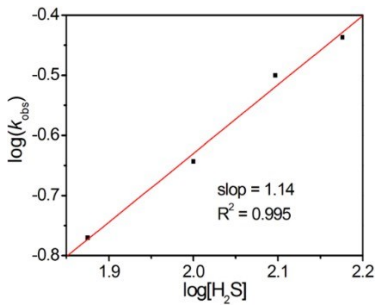

Fig. S12 The linear-relationship plot of log(k_{obs}) versus log([H_2S]). The slope of 1.14 supports the first-order dependence in H_2S for the thiolysis of **NBD-PZ-TPP**.

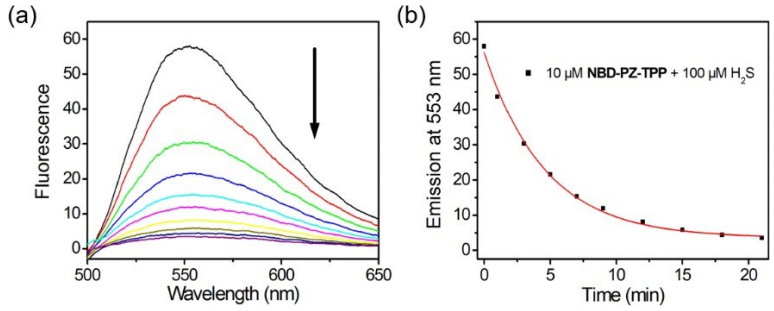

Fig. S13 (a) Time-dependent emission spectra of 10 μM **NBD-PZ-TPP** towards 100 μM H_2S in PBS buffer (50 mM, pH = 7.4) at 25 °C. (b) Time -dependent emission signals at 553 nm of 10 μM **NBD-PZ-TPP** towards 100 μM H_2S in PBS buffer (50 mM, pH = 7.4) at 25 °C . The pseudo-first-order rate, k_{obs} was determined by fitting the fluorescence intensity data with a single exponential function (red solid lines). The k_{obs} for **NBD-PZ-TPP** is 0.222 min^{-1} in the precence of 100 μM H_2S, which is close to the k_{obs} (0.227 min^{-1}) determined by monitoring changes in UV absorption in same conditions.

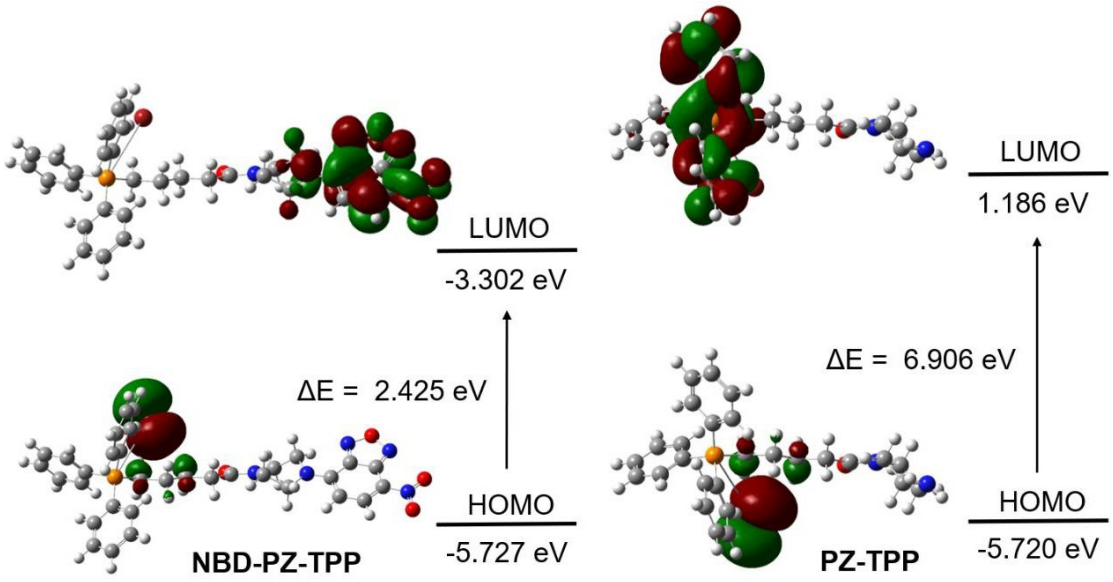

Fig. S14 Frontier orbital energy of **NBD-PZ-TPP** and the **PZ-TPP** moiety. Data were calculated by Gaussian 09 with B3LYP/6-31G(d) level.[4]

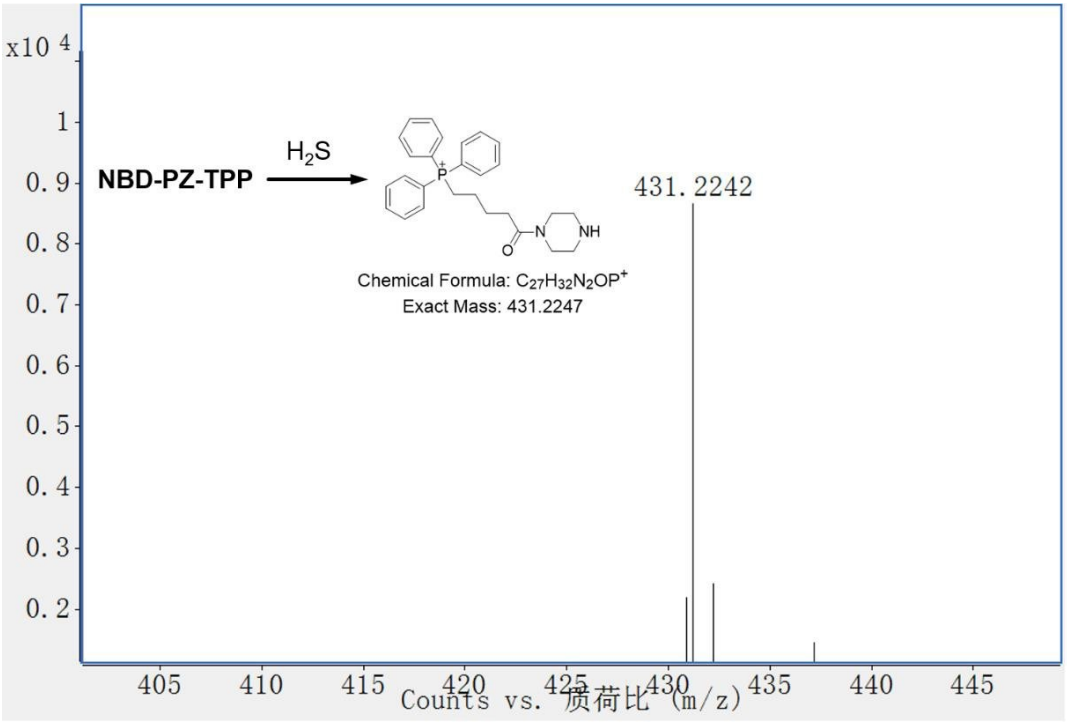

Fig. S15 HRMS spectra of the reaction of probe **NBD-PZ-TPP** (2 mM) with H_2S (5 mM) for 2 h in PBS buffer (pH = 7.4).

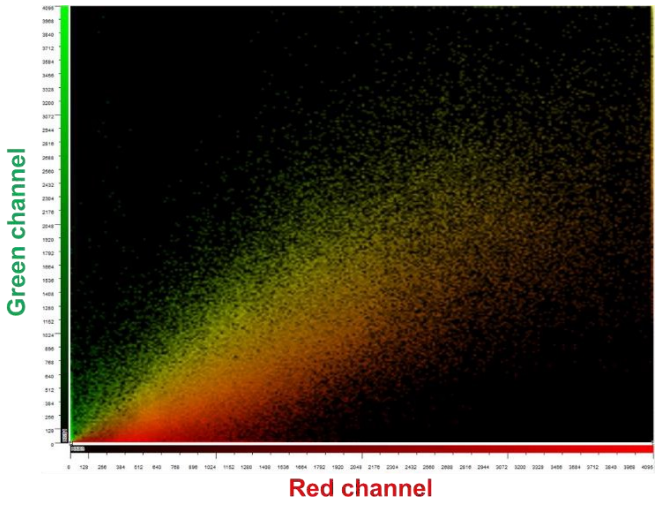

Fig. S16 Colocalization correlation scatter plots from Fig. 6.

9. Supplementary NMR and HRMS spectra

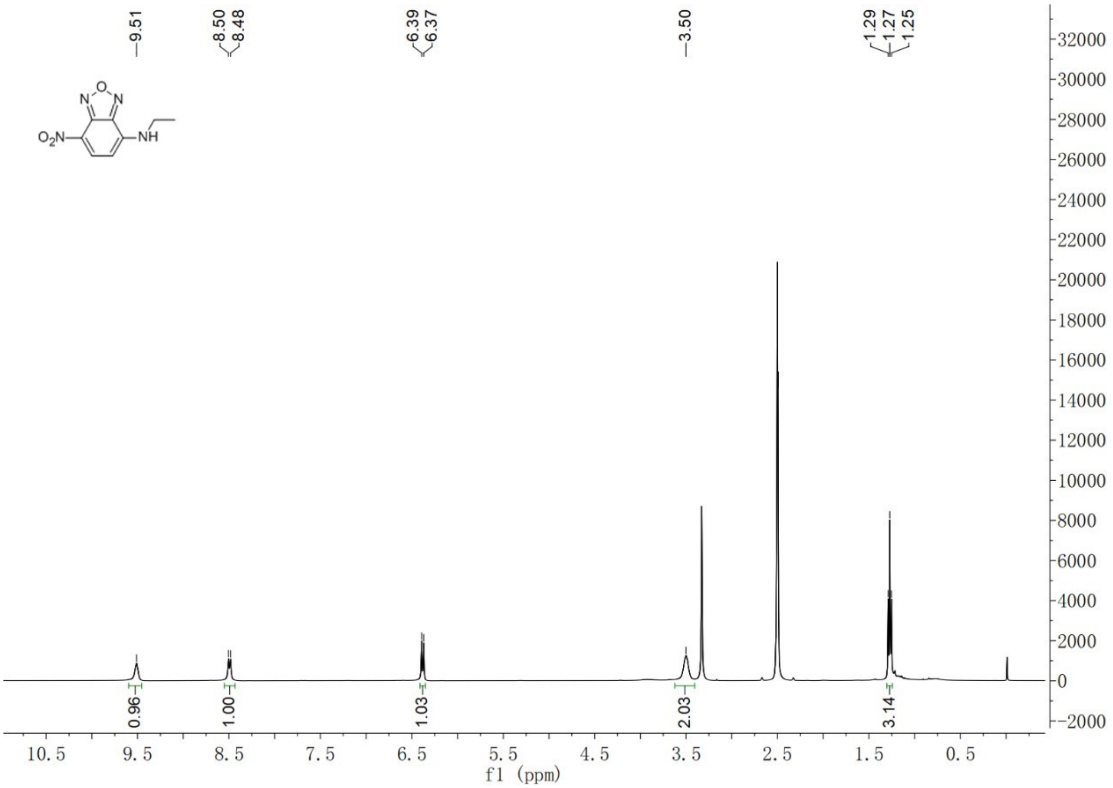

Fig. S17 ^{1}H NMR spectrum of **NBD-NHEt**.

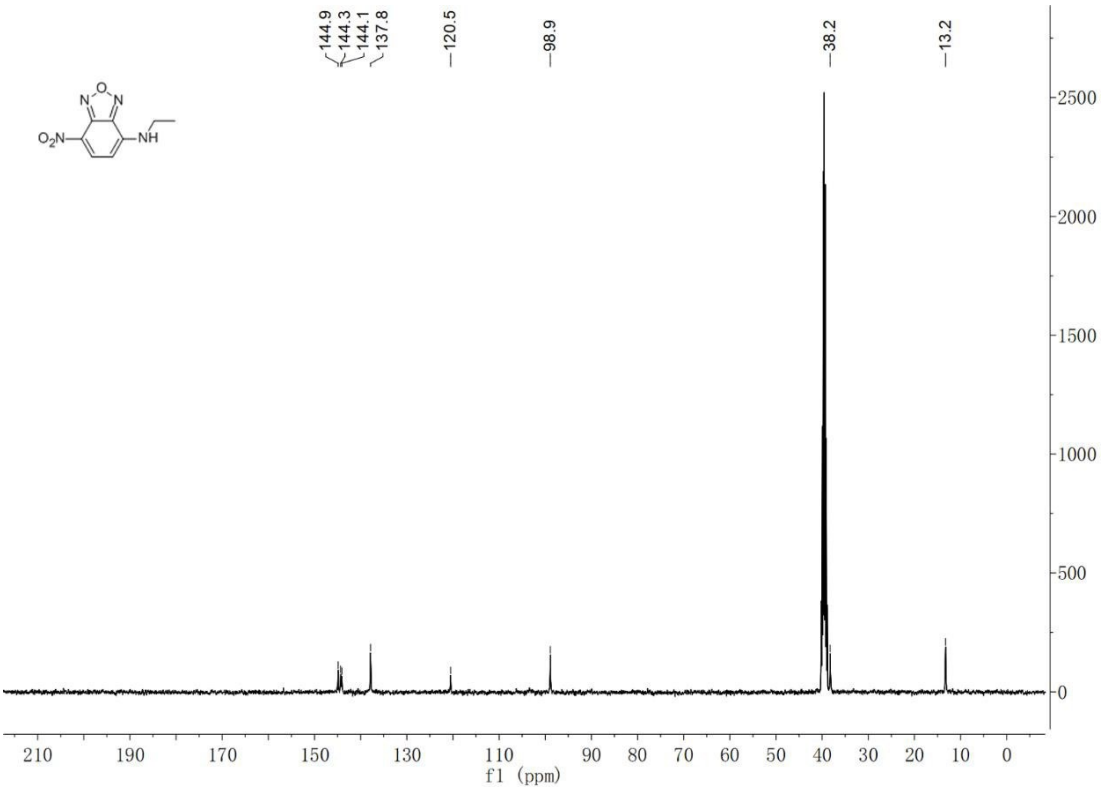

Fig. S18 ^{13}C NMR spectrum of **NBD-NHEt**.

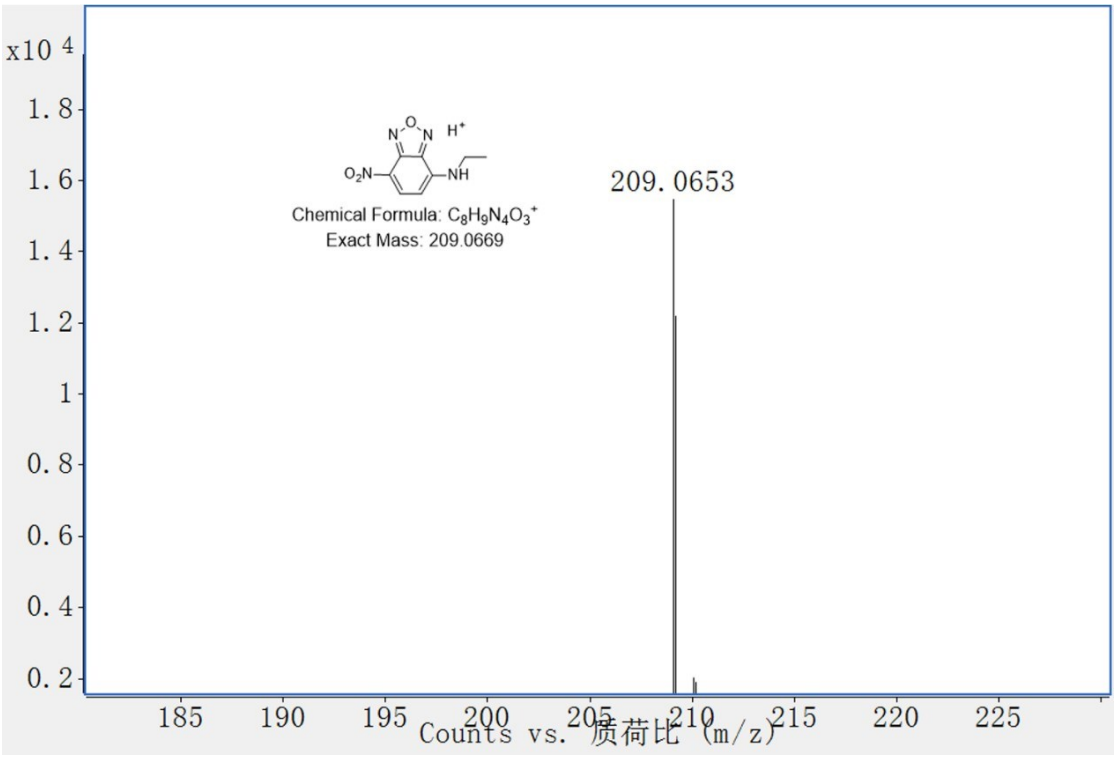

Fig. S19 HRMS spectrum of **NBD-NHEt**.

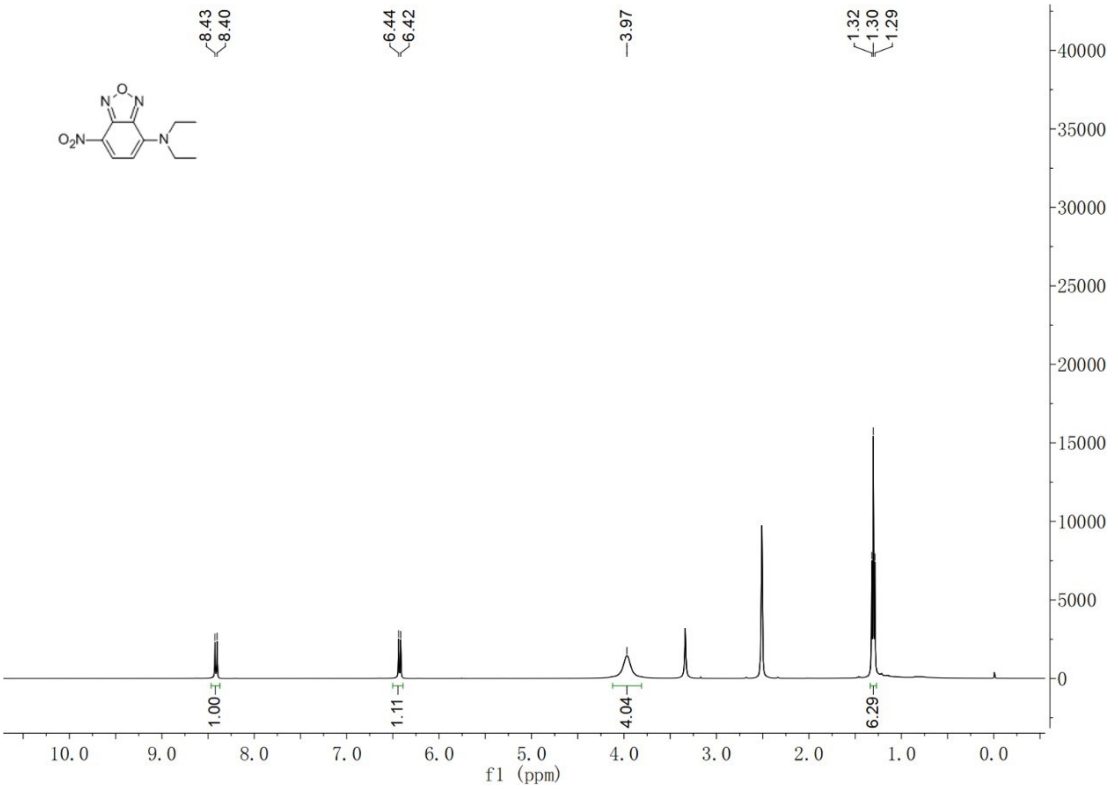

Fig. S20 ^{1}H NMR spectrum of **NBD-N(Et)$_2$**.

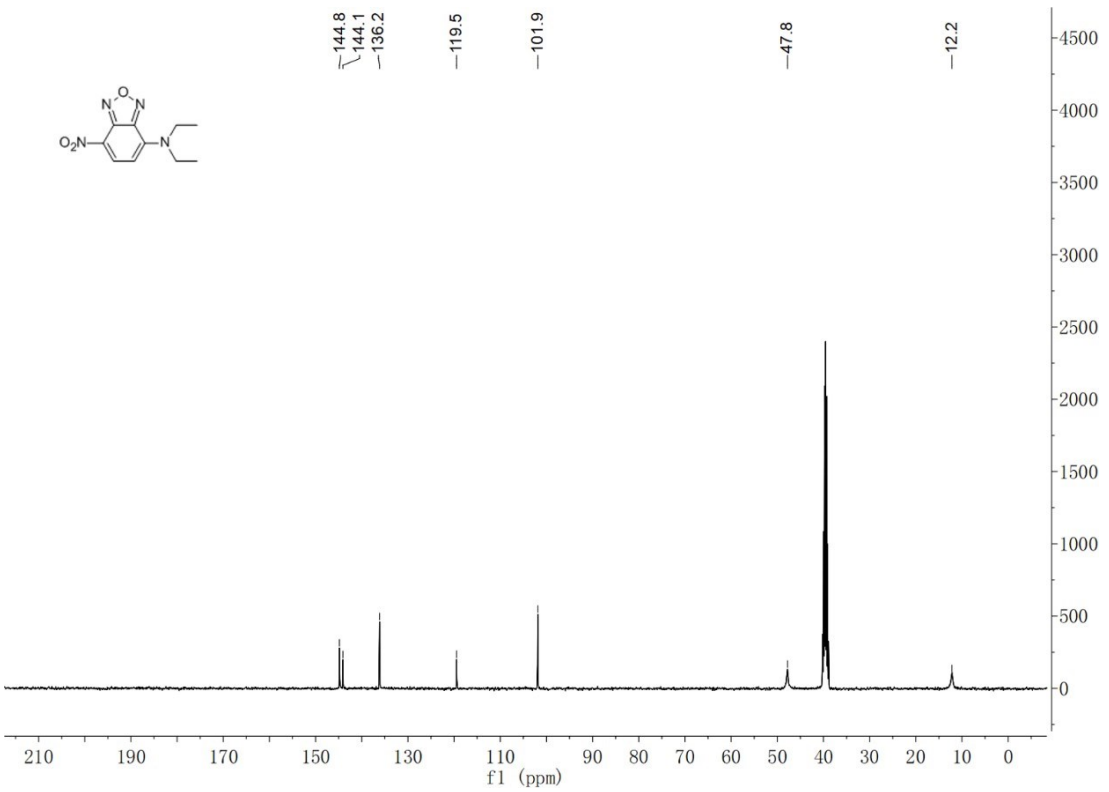

Fig. S21 ^{13}C NMR spectrum of **NBD-N(Et)$_2$**.

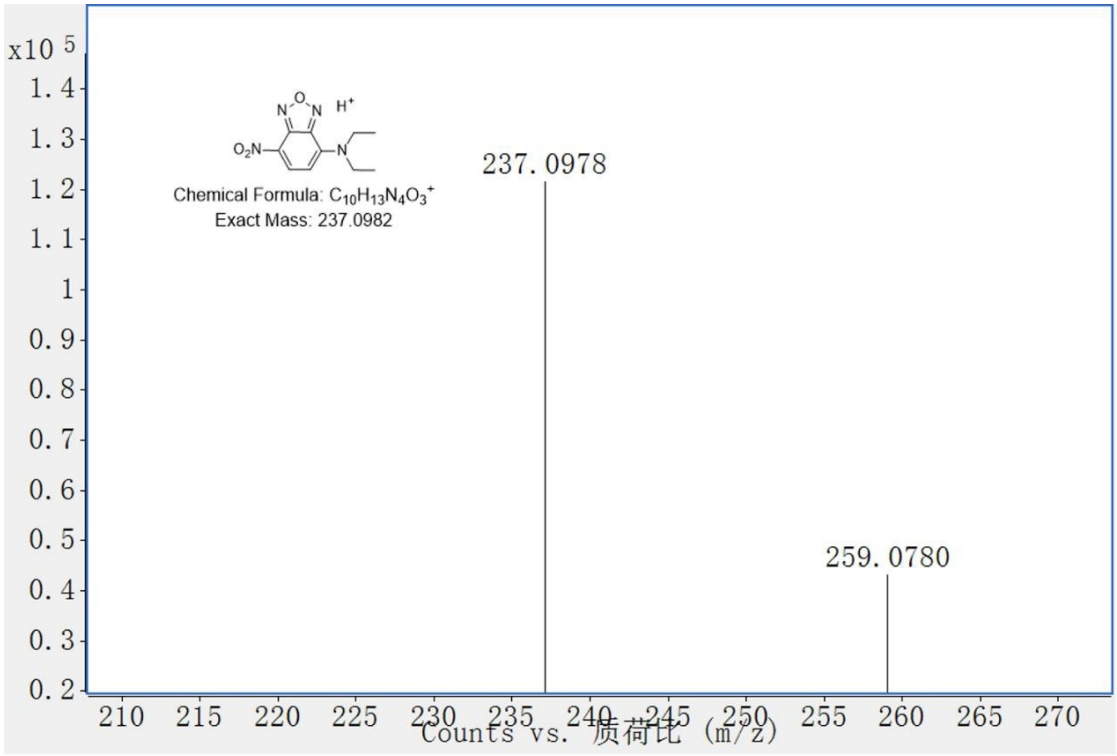

Fig. S22 HRMS spectrum of **NBD-N(Et)$_2$**.

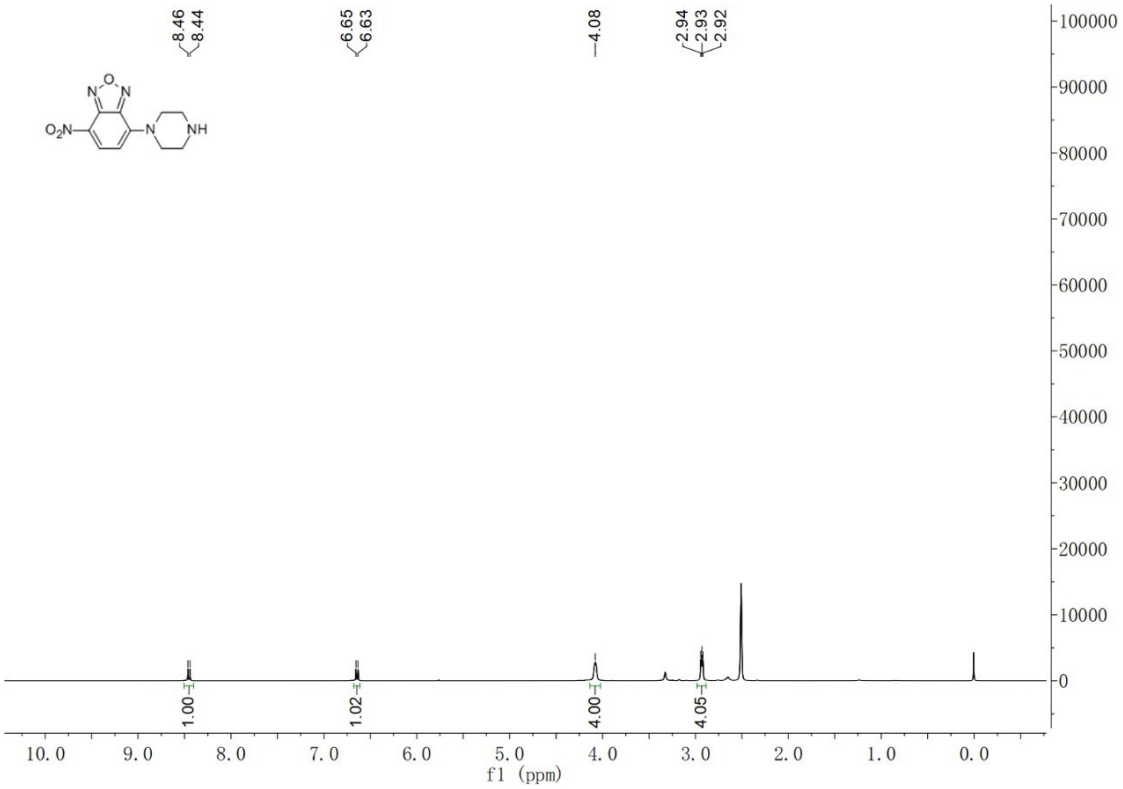

Fig. S23 ^{13}H NMR spectrum of **NBD-PZ**.

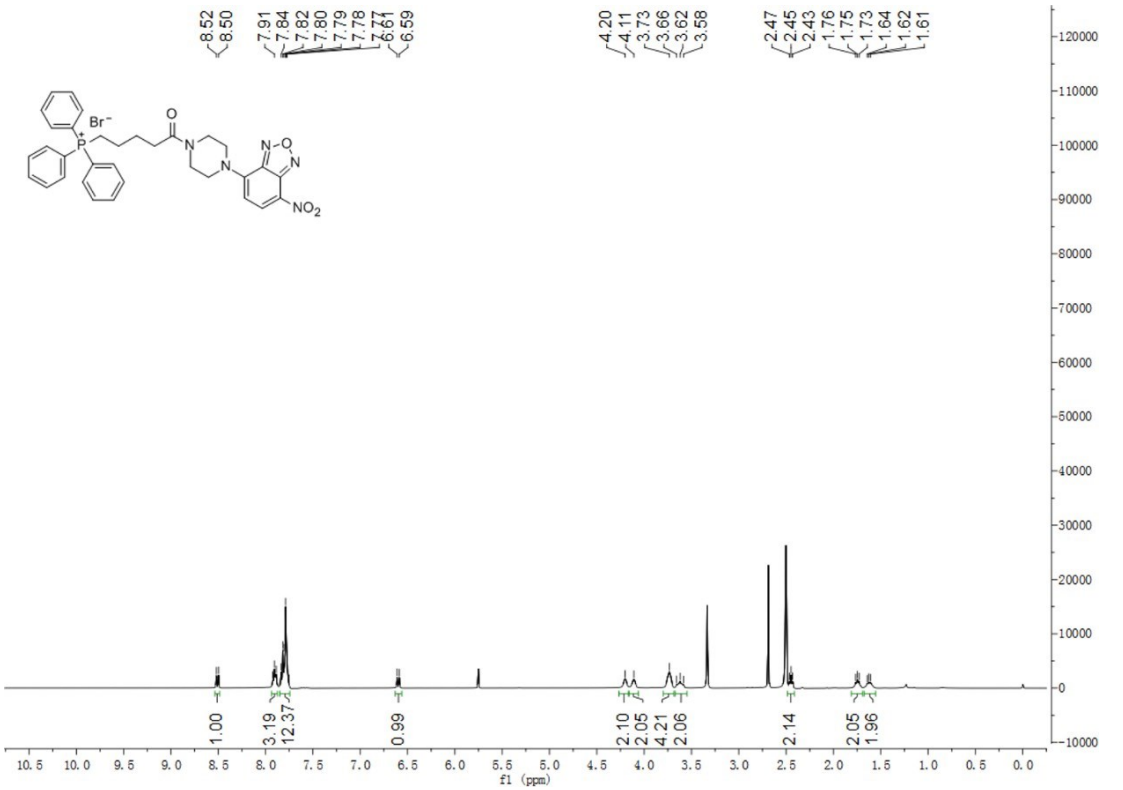

Fig. S24 ^{1}H NMR spectrum of **NBD-PZ-TPP**.

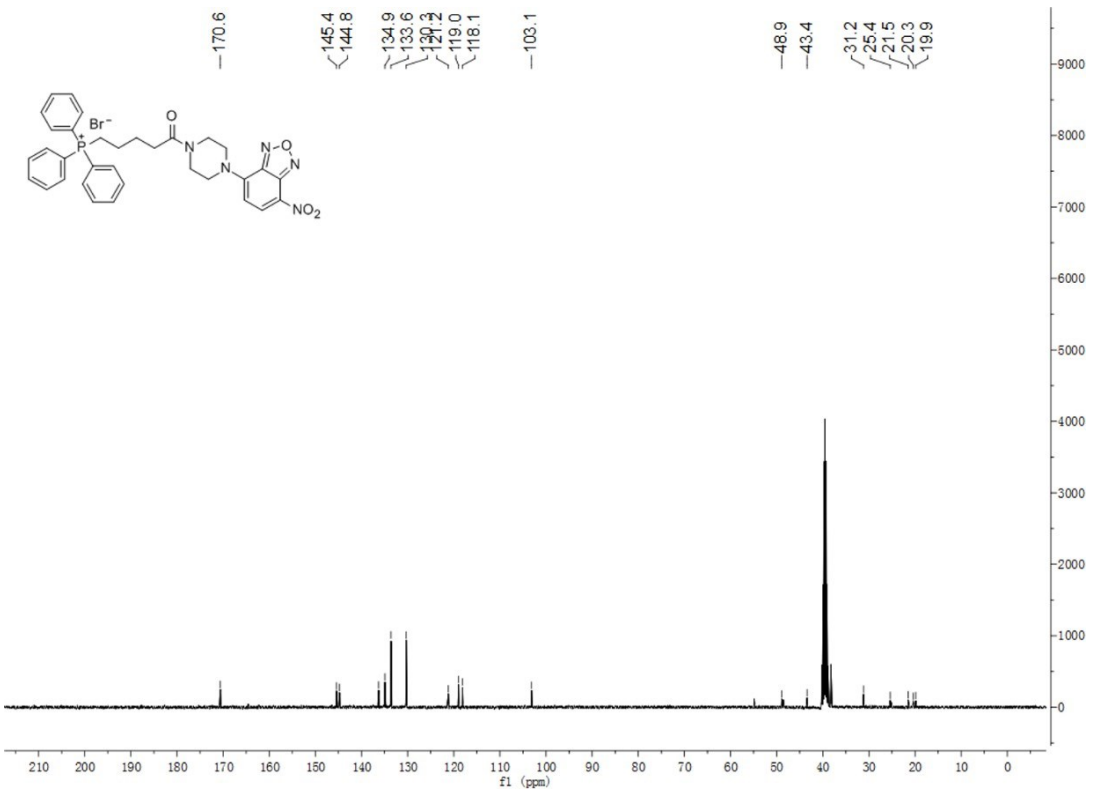

Fig. S25 ^{13}C NMR spectrum of **NBD-PZ-TPP**.

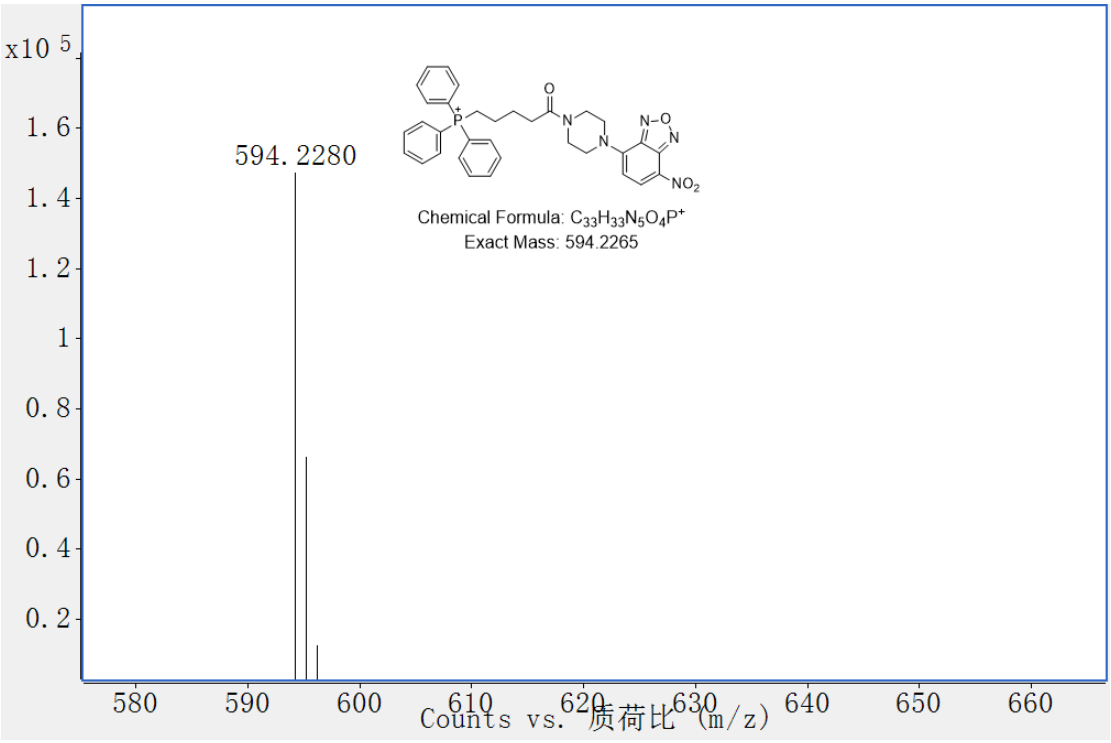

Fig. S26 HRMS spectrum of **NBD-PZ-TPP**.

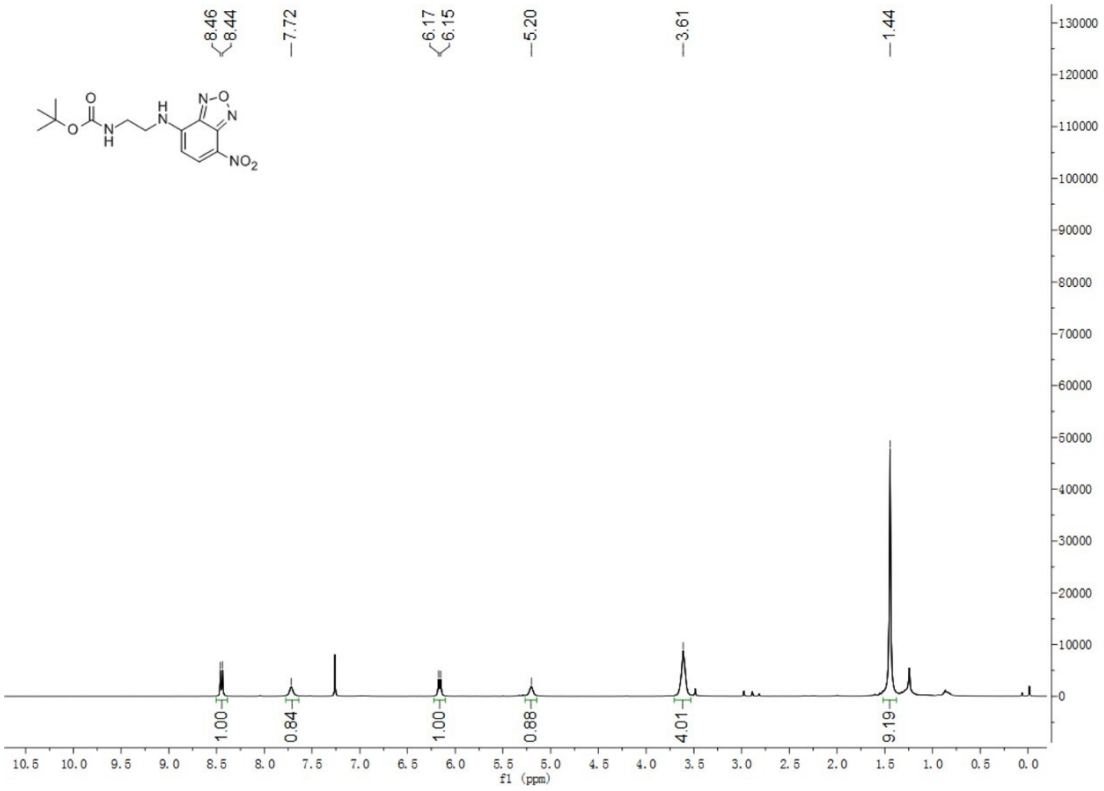

Fig. S27 ^{1}H NMR of **NBD-NH-Boc**.

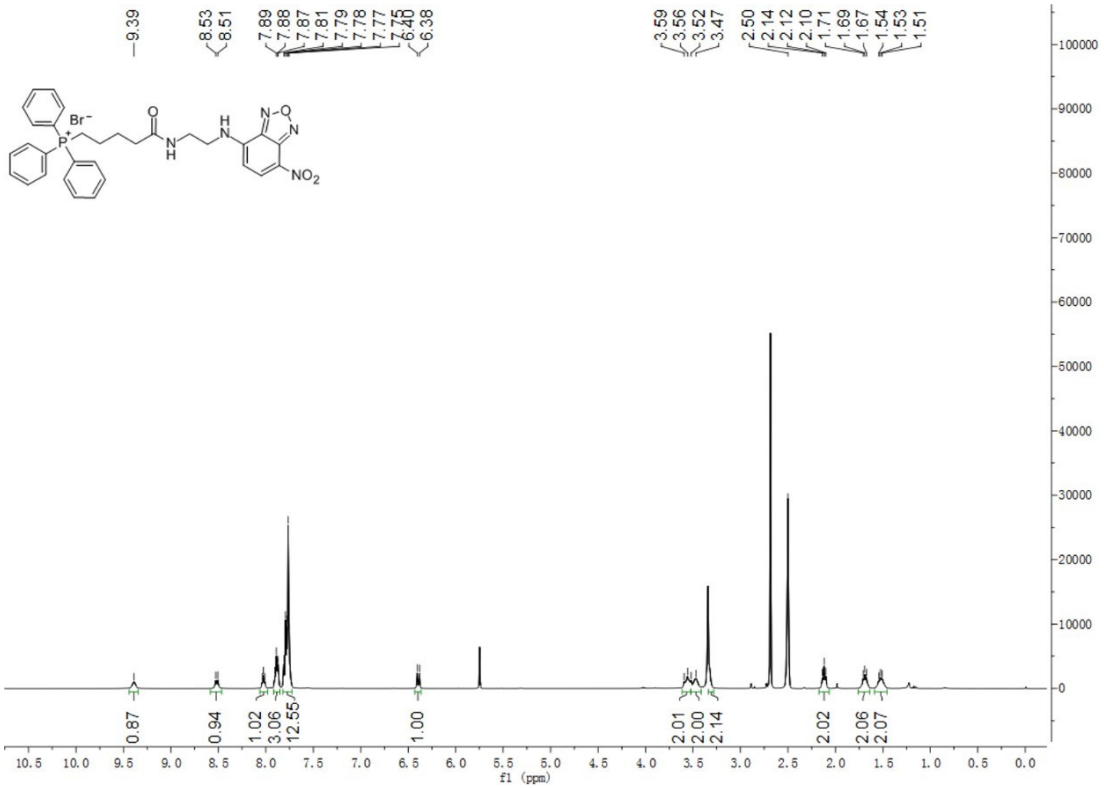

Fig. S28 ^{1}H NMR spectrum of **NBD-NH-TPP**.

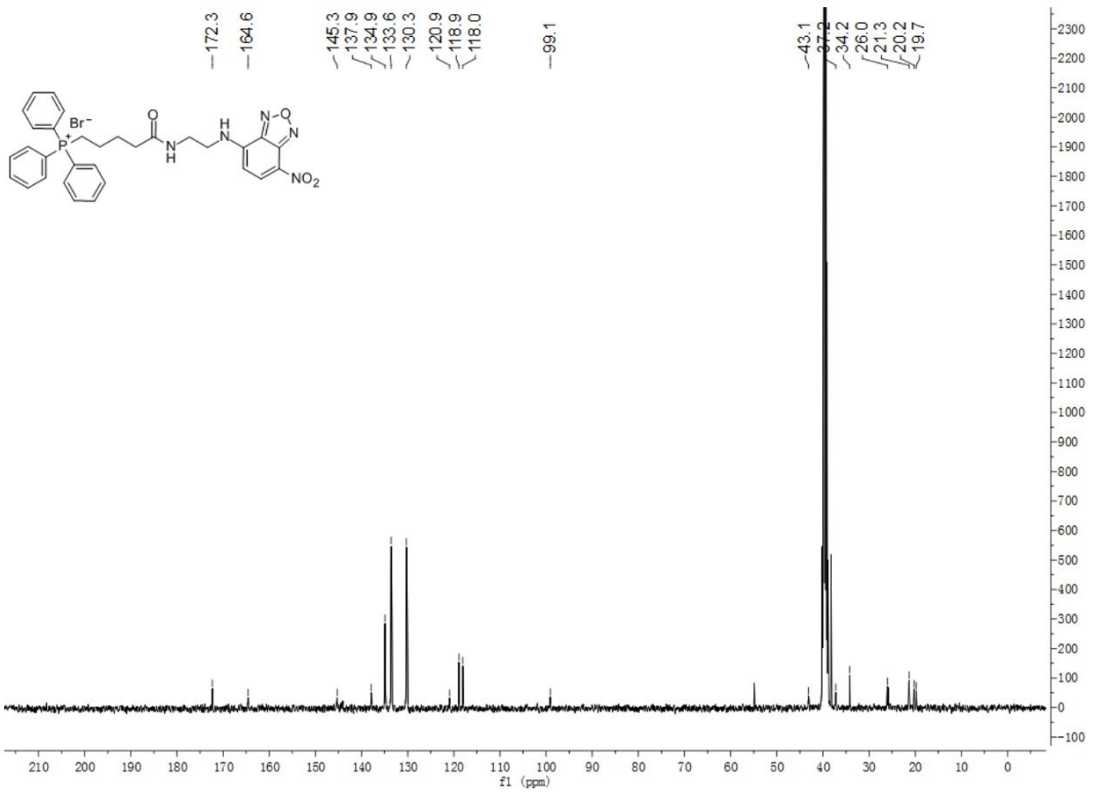

Fig. S29 ^{13}C NMR spectrum of **NBD-NH-TPP**.

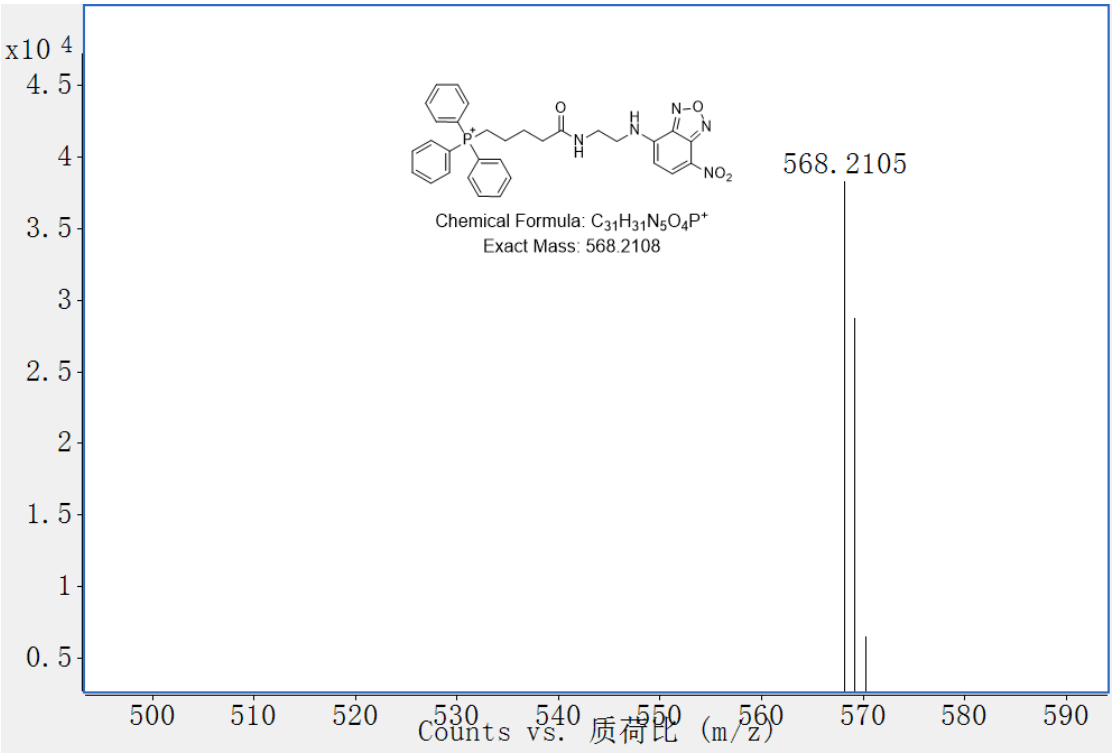

Fig. S30 HRMS spectrum of **NBD-NH-TPP**.

10. References

1. F. Song, Z. Li, J. Li, S. Wu, X. Qiu, Z. Xi and L. Yi, *Org. Biomol. Chem.*, 2016, **14**, 11117-11124.

2. S. K. Bae, C. H. Heo, D. J. Choi, D. Sen, E.-H. Joe, B. R. Cho and H. M. Kim, *J. Am. Chem. Soc*., 2013, **135**, 9915-9923.

3. S. Singha, D. Kim, B. Roy, S. Sambasivan, H. Moon, A. S. Rao, J. Y. Kim, T. Joo, J. W. Park, Y. M. Rhee, T. Wang, K. H. Kim, Y. H. Shin, J. Jung and K. H. Ahn, *Chem. Sci.*, 2015, **6**, 4335-4342.

4. M. Caricato, G. W. Trucks, M. J. Frisch and K. B. Wiberg, *J. Chem. Theory Comput.*, 2010, **6**, 370-383.